http://eprints.gla.ac.uk/4944/

Deposited on: 20 February 2009

Accepted Manuscript

Protein disulfide isomerase activity is essential for viability and extracellular matrix formation in the nematode *Caenorhabditis elegans*

Alan D. Winter, Gillian McCormack, Antony P. Page

Please cite this article as: Winter, Alan D., McCormack, Gillian, Page, Antony P., Protein disulfide isomerase activity is essential for viability and extracellular matrix formation in the nematode *Caenorhabditis elegans*, *Developmental Biology* (2007), doi: 10.1016/j.ydbio.2007.05.041

Protein disulfide isomerase activity is essential for viability and extracellular matrix formation in the nematode *Caenorhabditis elegans*.

Alan D. Winter[1], Gillian McCormack[1] and Antony P. Page[1]*

[1]Institute of Comparative Medicine, Veterinary Faculty, University of Glasgow, Bearsden Road, Glasgow, G61 1QH, Scotland, United Kingdom.

*Corresponding author: a.page@vet.gla.ac.uk

Institute of Comparative Medicine, Veterinary Faculty, University of Glasgow,

Bearsden Road, Glasgow, G61 1QH, Scotland, United Kingdom.

Tel. 0044 1413301997 Fax. 0044 1413305603

Abstract

Protein disulfide isomerase (PDI) is a multifunctional protein required for many aspects of protein folding and transit through the endoplasmic reticulum. A conserved family of three PDIs have been functionally analysed using genetic mutants of the model organism *Caenorhabditis elegans*. PDI-1 and PDI-3 are individually non-essential, whereas PDI-2 is required for normal post-embryonic development. In combination, all three genes are synergistically essential for embryonic development in this nematode. Mutations in *pdi-2* result in severe body morphology defects, uncoordinated movement, adult sterility, abnormal molting and aberrant collagen deposition. Many of these phenotypes are consistent with a role in collagen biogenesis and extracellular matrix formation. PDI-2 is required for the normal function of prolyl 4-hydroxylase, a key collagen-modifying enzyme. Site-directed mutagenesis indicates that the independent catalytic activity of PDI-2 may also perform an essential developmental function. PDI-2 therefore performs two critical roles during morphogenesis. The role of PDI-2 in collagen biogenesis can be partially restored following complementation of the mutant with human PDI.

Introduction

Protein folding requires the assistance of catalysts to accelerate the attainment of native conformation and chaperones to prevent misfolding and aggregation. Disulfide bond formation is the key step in the stability and proper function of numerous proteins. The enzyme protein disulfide isomerase (PDI, EC 5.3.4.1), identified more than 40 years ago (Goldberger et al., 1964), performs the critical role of native disulfide bond formation in the cell. PDI catalyses the formation (oxidation), breakage (reduction) and rearrangement (isomerisation) of disulfide bonds within proteins, thereby permitting their proper folding in the endoplasmic reticulum (ER) and transit through the secretory pathway (Ellgaard and Ruddock, 2005; Gething and Sambrook, 1992).

PDI has a multi-domain structure consisting primarily of two active, *a* and *a'*, and two inactive, *b* and *b'*, thioredoxin domains, with the homologous *a* and *a'* domains of PDI each containing the defining CxxC active site of these enzymes (Darby et al., 1998; Kemmink et al., 1997). The *b'* domain is the principal substrate binding site with specific mutations in a small hydrophobic pocket affecting substrate binding (Pirneskoski et al., 2004). While simple isomerisation reactions can be accomplished with one catalytic domain in combination with the *b'* domain, where isomerisation is linked to a significant change in substrate structure, all domains are required for full enzymatic activity (Darby et al., 1998). The specific order of the domains within PDI allows for the dual activity of this enzyme, as a disulfide isomerase and a disulfide oxidase, by establishing an asymmetry in oxidation rates between the two active sites (Kulp et al., 2006). Recent structural determination of yeast Pdi1p confirms the functional requirement for all domains, with the apposing active sites forming part of a continuous hydrophobic surface that interacts with the

substrate and facilitates oxidase, isomerase and chaperone functions (Tian et al.,

2006).

PDI is a multi-functional enzyme that, in addition to its independent enzymatic

activity in protein folding, is a subunit of collagen prolyl 4-hydroxylase (P4H, EC

1.14.11.2) and microsomal triglyceride transfer protein complexes (Myllyharju and

Kivirikko, 2004; Wilkinson and Gilbert, 2004). P4H catalyses the critical step of

hydroxylating proline residues in the X-Pro-Gly repeat sequences of collagens. In

most species examined P4H complexes are $\alpha_2\beta_2$ tetramers with PDI representing the

β subunits and catalytic activity residing in the α subunits (Myllyharju and Kivirikko,

2004). The role of PDI in P4H complexes is independent of its catalytic activity since

active site mutants of PDI can form fully active P4H tetramers (Vuori et al., 1992).

PDI functions within the P4H complex to keep the active subunits soluble and in a

catalytically active confirmation, a role that cannot be substituted for by the

chaperones ERp57/60 or BiP (Koivunen et al., 1996). The *a′* and *b′* domains of PDI

fulfil the minimum requirement to serve as a P4H subunit but all four domains greatly

enhance assembly into tetramers (Pirneskoski et al., 2001), with binding sites in the *a*,

b′ and *a′* domains contributing to complex assembly (Koivunen et al., 2005). An ER

retention signal at the C-terminus of PDI serves to maintain the P4H complexes in the

correct sub-cellullar compartment (Vuori et al., 1992). In addition to modified proline

residues, collagens also contain disulfide linkages such as the intra- and inter-

molecular bonds between conserved cysteine residues in the vertebrate fibrillar

collagens (Bulleid, 1996). Therefore, in addition to the collagen related function of

PDI in P4H complex formation, PDI is hypothesized to have an independent

enzymatic role during collagen biosynthesis.

4

The nematode *Caenorhabditis elegans* provides a genetically amenable system in which to study PDI function in the context of extracellular matrix (ECM) formation. ECMs in all animals are composed primarily of collagens that are assembled via a number of intra- and extra-cellular enzymatic modifications (Page and Winter, 2003). Nematodes have two forms of ECM, the cuticle that covers the outermost epithelial cells and functions as an exoskeleton and the basement membranes that cover most internal organs. The *C. elegans* cuticle is constructed from multiple collagenous layers that contain extensive disulfide linkages (Cox et al., 1981). Five cuticles are synthesised throughout *C. elegans* development, the first at the end of embryogenesis and thereafter a new cuticle is produced for each of the subsequent developmental stages. The essential role of the cuticle in body shape maintenance is highlighted by mutations in cuticle collagens or collagen enzymes that produce drastically altered body morphologies and lethality (Kramer, 1997; Page and Winter, 2003).

The *C. elegans* genome has three conserved PDI encoding genes, namely *pdi-1* (Veijola et al., 1996), *pdi-2* (Winter and Page, 2000) and *pdi-3* (Eschenlauer and Page, 2003), and a greater number of proteins with thioredoxin domains which are targeted to the ER. Recombinant expression demonstrates that all three PDIs are active disulfide isomerases and in addition show transglutaminase-like cross-linking activity (Eschenlauer and Page, 2003). Co-expression studies in insect cells reveal that PDI-2, but not PDI-1 or PDI-3, can form active P4H enzyme complexes when expressed in combination with α subunits (Myllyharju et al., 2002), (Page unpublished observations). *pdi-2* is expressed in the hypodermis, the cuticle collagen synthesising tissue, at times of maximal collagen production (Myllyharju et al., 2002; Winter and Page, 2000). This expression pattern mirrors that of the collagens

5

themselves (Johnstone and Barry, 1996; McMahon et al., 2003) and the P4H α

subunit encoding genes *dpy-18* (*phy-1*) and *phy-2* (Myllyharju et al., 2002; Winter and

Page, 2000). Simultaneous removal of *dpy-18* and *phy-2* by a combination of mutant

and RNA interference (RNAi) analysis results in embryonic lethality in *C. elegans*

and is phenocopied upon disruption of *pdi-2* by RNAi (Winter and Page, 2000). Time-

course analysis indicates that embryos elongate normally until the point at which the

cuticular exoskeleton is required to maintain this morphology (Winter and Page,

2000).

The detailed genetic analysis of PDI and thioredoxin function has to date been

performed predominantly in yeast and bacteria (Wilkinson and Gilbert, 2004) and the

relationship to P4H function, collagen biogenesis and ECM formation therefore has

not been addressed. This study analyses the function of the conserved PDI family of

enzymes in *C. elegans*, defines their distinct roles in ECM formation and examines

their overlapping functions.

Materials and Methods

C. elegans **strains and culture conditions.** The following *C. elegans* strains

were received from the *Caenorhabditis* Genetic Centre; N2 (wild type), NL2099 [*rrf-

3*(*pk1426*) II], VC858 {+/szT1[*lon-2*(*e678*)] I; *pdi-2*(*gk375*)/szT1 X}, CB678 [*lon-

2*(*e678*) X], JK2757 [*phy-2*(*ok177*) IV], CB2590 [*tra-1*(*e1099*)/*dpy-18*(*e1096*) III],

CB4121 [*sqt-3*(*e2117*) V], BE63 [*sqt-3*(*sc63*) III], CB88 [*dpy-7*(*e88*) X], CB164

[*dpy-17*(*e164*) III] and CB364 [*dpy-18*(*e364*) III]. *sqt-3*(*e2924*) and *dpy-31*(*e2770*)

were obtained form J. Hodgkin (Oxford). Nematodes bearing the *pdi-2*(*tm0689*)

deletion allele were produced by the National Bio-Resource Project for the Nematode

(Japan). An out-crossing regime and multiplex single worm PCR strategy were

employed to remove undesirable mutations while maintaining the *pdi-2*(*tm0689*) deletion allele. *tm0689* was out-crossed four times with the wild type N2 strain, then with CB678 to introduce a marker chromosome containing *lon-2*(*e678*) in *trans* to *pdi-2*(*tm0689)* to generate TP69 [*pdi-2*(*tm0689*)/*lon-2*(*e678*) X]. Strain TP91 [*pdi-2*(*gk375*)/*lon-2*(*e678*) X] was generated by first out-crossing VC858 with wild type N2 animals then with CB678. *C. elegans* strains TP67 [*pdi-1*(*ka3*) III] and TP66 [*pdi-3*(*ka1*) I] were produced as described in the deletion library screen section. Strains TP72 [*pdi-3*(*ka1*) I; *pdi-1*(*ka3*) III], TP84 [*pdi-1*(*ka3*) III; *pdi-2*(*tm0689*) X], TP85 [*pdi-3*(*ka1*) I; *pdi-2*(*tm068*) X] and TP96 [*pdi-3*(*ka1*) I; *pdi-1*(*ka3*) III; *pdi-2*(*tm0689*) X] were made by performing standard genetic crosses and genotyped by PCR. TP75 [*pdi-3*(*ka1*) I; *sqt-3*(*e2117*) V], TP76 [*pdi-3*(*ka1*) I; *sqt-3*(*e2924*) V], TP77 [*pdi-3*(*ka1*) I; *dpy-17*(*e164*) III], TP78 [*pdi-3*(*ka1*) I; *dpy-18*(*e364*) III], TP79 [*pdi-3*(*ka1*) I; *dpy-31*(*e2770*) III], TP94 [*pdi-3*(*ka1*) I; *sqt-3*(*sc63*) III] and TP95 [*pdi-3*(*ka1*) I; *dpy-7*(*e88*) X] were made by performing standard genetic crosses with the relevant strains. Strains were genotyped for *pdi-3* using multiplex single worm PCR and other genotypes determined by segregation of progeny. Strains that displayed an increase in severity were maintained as *pdi-3* homozygotes and were heterozygotic for the additional mutation. A double genetic knockout of *dpy-18* and *phy-2* (TP92) was produced by crossing two null deletion alleles, *dpy-18*(*e1096*) III with JK2757 [*phy-2*(*ok177*) IV], and was assessed by PCR. All genotyping primers and the multiplex single worm PCR methods are described in the supplemental material.

Mutant library screen for *pdi-1* and *pdi-3* deletion alleles. A randomly mutagenized population of *C. elegans* was produced by UV/ trimethylpsoralen and screened by multiplex PCR to identify populations carrying deletions in target genes. The deletion library was constructed and screened essentially as described previously

7

(Barstead, 1999). Primer sequences used to identify and characterize the deletion alleles are available on request and those used for out-crossing to produce the TP67 [*pdi-1*(*ka3*)] and TP66 [*pdi-3*(*ka1*)] deletion strains are presented in the supplemental material, with four outcrosses performed for each.

Transgenic expression of *C. elegans pdi-2*. Vector pAW2 was designed for expression of *pdi* coding sequences in *C. elegans* and contained *pdi-2* promoter sequences from -2620 to +5 (relative to ATG) (Winter and Page, 2000) (full details in supplemental material). Site-directed mutagenesis was performed on the wild type clone of *pdi-2* in vector pAW2 to generate mutations in the active sites. A QuikChange Site-Directed Mutagenesis kit (Stratagene) was employed following the manufacturer's recommendations, with the mutagenesis carried out in two steps each altering the pair of cysteine residues from the two active sites of PDI-2 (detailed methods are listed in supplemental material). Rescue and mutagenesis expression constructs were microinjected at a concentration of 10-25 μg/ml into the strain TP69. A marker plasmid, containing the promoter region of the cuticle collagen gene *dpy-7* driving expression of GFP in the vector pPD95.67, was co-injected at 5 μg/ml with the final concentrations of the injection mix increased to 150 μg/ml with pBluescript SKM (Stratagene). Phenotypically wild type animals from the strain TP69 represented *pdi-2*(*tm0689*)/*lon-2*(*e678*) heterozygotes that were selected for injection with transformed progeny identified by expression of GFP via UV microscopy.

Primers employed for genotyping and RT-PCR of transgenic strains are described in the supplemental material. The genotyping primers were re-designed to specifically amplify from chromosomal and not transgenic template when the injected plasmid contained *pdi-2* sequences. RT-PCR was performed on mixed stage cDNA

8

from semi-stable transgenic lines and from the strain TP69. To detect expression of

transgenic *pdi-2* sequences in *C. elegans* the difference in 3'UTR regions between

transgene and chromosomal *pdi-2* was utilised to selectively amplify from transgene-

derived material.

  Transgenic expression of human *PDI*. Full details for the construction of

human PDI transgenic constructs are listed in the supplemental material. Rescue and

marker plasmids were linearised with blunt cutting enzymes that cut singly in the

plasmid backbones. The human *PDI* rescue clone was linearised with *Eco* RV, *Fsp* I

was used for the *dpy-7*GFP marker plasmid and *Pvu* II for the *C. elegans* genomic

DNA. Plasmid DNA was purified using QIAquick PCR purification kit (Qiagen) and

genomic DNA was purified by phenol/chloroform extractions and ethanol

precipitation. Plasmids were microinjected at 2 μg/ml together with 100 μg/ml

genomic DNA into TP69 as described above. Details of genotyping and RT-PCR of

transgenic lines are described in the supplemental material.

  To confirm that human *PDI* was responsible for the rescue, sequences from

this gene were used to perform RNAi by bacterial feeding (Kamath et al., 2003).

Rescued homozygous mutants were grown on plates with the human *PDI* dsRNA

expressing cells and were compared to controls grown on plates with cells containing

vector alone.

  RNA interference of *pdi-2* and *pdi*-like genes. The inhibitory activity of *pdi-2* RNAi constructs containing the full-length gene (Winter and Page, 2000) or exon

three only (Kamath et al., 2003) were assessed via injection and bacterial feeding

methods (Kamath et al., 2003; Winter and Page, 2000). The effect of disruption of an

additional two *pdi*-like genes present in the *C. elegans* genome were examined using

the bacterial feeding method with clones from the RNAi feeding library (Kamath et

9

al., 2003) representing genes B0403.4 (NM_076789) and C14B9.2 (NM_066374).

These were used to disrupt gene function in the wild type (N2) strain, an RNAi

hypersensitive strain (NL2099), and the *pdi* mutants TP66, TP67, TP69, TP72 and

TP91.

Western Blotting. SDS PAGE gels and protein transfer was performed as

described previously, blots being probed with an anti-PDI-2 polyclonal antibody

(Myllyharju et al., 2002). 100 adult stage nematodes of wild type, *pdi-2* mutant,

transgene rescue, and transgenic active-site mutants were picked individually into

100µl of M9 buffer, allowed to settle, centrifuged, re-suspended in 30µl of ST buffer

(1% SDS, 0.125M Tris PH 6.8) and frozen at -80°C. Samples were manually

homogenized, boiled for 10 mins in 5% β-mercaptoethanol, SDS PAGE loading

buffer and 15µl of the centrifuged supernatant was loaded per well onto a 4-12%

precast SDS PAGE MOPs gel (Invitrogen).

Microscopy. Live nematodes were transferred to a 2% agarose pad on a

slide (with 0.065% sodium azide) and the coverslip sealed with white paraffin.

Nematodes that were prone to burst due to a weakened cuticle were transferred to a

solution of 1% gluteraldehyde on the agarose pad (minus sodium azide) .

Immunocytochemistry was carried out as described previously (Eschenlauer and

Page, 2003), using anti-DPY-7 monoclonal antibody and Alexa Fluor 488 anti-mouse

secondary antibody (Molecular Probes). Images for both Nomarski and

immunofluoresence microscopy were captured digitally using an Axioskop 2 Plus

microscope (Zeiss) using Axiovision (Zeiss) or OpenLab (Improvision) software.

Scanning electron microscopy was carried out as described previously (Eschenlauer

and Page, 2003). TEM samples were fixed in 2.5% gluteraldehyde then 1% osmium

tetroxide in 0.1M phosphate buffers. Samples were dehydrated and infiltrated in LR-

White resin (Page et al., 1992) and viewed on a Leo 912AB microscope. All figures

were assembled using Adobe Photoshop.

Results

        ***pdi-1* and *-3* are dispensable for nematode viability while *pdi*-2 is**

essential for normal development. Genetic mutants of the three conserved PDI

encoding genes *pdi-1, -2* and *-3* were obtained by random mutagenesis and PCR

screening. Following backcrossing and sequencing, the positions of the deletions

were mapped and shown to affect functional domains in all three PDI enzymes (Fig.

1). A 732 bp deletion allele, *pdi-1*(*ka3*), was isolated which corresponded to co-

ordinates 1276/1277 - 2008/2009 with respect to cosmid C14B1 (accession number

Z37139). This resulted in an in-frame deletion that removed amino acids valine-7 to

threonine-218 and thereby affected the entire *a* and *b* domains (Fig. 1). Two

independent mutant alleles of *pdi-2* were obtained from the *C. elegans* knockout

consortia. Allele *tm0689* was a 551 bp deletion that corresponded to cosmid C07A12

(accession number U41542) co-ordinates 11825/11826-12376/12377. This allele

deleted amino acids asparagine-318 to leucine-388 and was predicted to result in a C-

terminal truncation affecting the *a'* domain and ER retention signal. The mutant allele

gk375 represented an 832 bp deletion in *pdi-2* (cosmid co-ordinates 10265/10266-

11097/11098). This removed the start methionine to lysine-158, encompassing the

signal peptide and the entire *a* domain (Fig. 1). A 436 bp deletion in the *pdi-3* gene,

allele *ka1*, (13963/13964 – 14399/14400 fosmid H06o01, accession number Z92970)

was isolated that removed amino acids threonine-282 to lysine-388 and covered large

portions of the *b'* and *a'* domains and spanned the second active site. This deletion

ended in an intron and was therefore predicted to result in a truncation (Fig. 1). The

11

mutant PDI proteins, if expressed, were predicted to be severely disrupted, or at the very least lacking in disulfide isomerase activities as all PDI domains are required for full enzymatic activity (Darby et al., 1998).

The *pdi* deletion strains were scored for embryonic lethality and assessed visually for post-embryonic arrest, growth, movement, and body morphology defects over a range of growth temperatures (Fig. 2 and Table 1). The homozygous deletion of *pdi-1* had no effect on nematode morphology (Fig. 2B), or indeed any of the characteristics scored (Table 1). The homozygous *pdi-3* mutants were likewise predominantly wild type with the exception that they displayed a mild dumpy (shorter and fatter than wild type) phenotype (Fig. 2D and Table 1). The phenotypes defined for the *pdi-1* and *pdi-3* mutants were in agreement with those described previously following RNAi analysis (Eschenlauer and Page, 2003; Kamath et al., 2003). In contrast, the *pdi-2* homozygotes displayed severely abnormal body morphologies; measuring approximately 390μm in early adult stages (Fig. 2C) down to 200μm in older adults (Fig. 2E and G), when compared to the 1000μm plus size of young wild type adults (Fig. 2A). The severity of the mutant phenotype was not temperature-dependant and no significant embryonic lethality was noted (Table 1). Homozygotes for both *pdi-2* alleles were separated from their mixed genotype strains to determine if they could generate viable progeny (n=>60 at 15, 20 and 25°C for each allele, total n=396). While a proportion did develop to adult stage, all were completely sterile. Additionally, mutants displayed a highly variable uncoordinated movement phenotype, the severity of which corresponded to the degree of body morphology defects, being most common in older adults. This phenotype was most probably a direct result of incomplete muscle attachments to the severely disrupted cuticle. As a consequence of their inviable and sterile phenotypes these alleles were maintained as

12

heterozygotes and this is reflected in the segregation ratios detailed in Table 1. The two *pdi-2* mutant alleles demonstrated a degree of variability but were morphologically indistinguishable from each other (data not shown), with the phenotype becoming more pronounced in later larval stages culminating in the late adult stages (Figs. 2E and G). The sterility of the mutants may in part be explained by the morphology of the hermaphrodite gonad, the development of which is highly constrained within the mutant body-form. The wild type hermaphrodite gonad forms two tubular U-shaped arms, each proximally terminating at a spermatheca (Kimble and Ward, 1988). The gonads in *pdi-2* homozygous mutant adults were short, displaced and not fully differentiated; no spermatheca, oocytes or embryos were observed in any adults examined. The distal regions containing syncytial nuclei were however clearly discernable in these mutants (Fig. 2E-H). In addition, the vulva was noted as being enlarged and gaping (Fig. 2H), in some individuals, the internal contents including the gonads were extruded through the abnormal vulval opening (data not shown). It is however, interesting to note that organs such as the muscular pharynx developed normally, but were highly folded and displaced, again being restricted by the mutant cuticle and the associated constrained body form (Fig. 2E and G). Both strains also exhibited widespread molt defects, characteristically retaining un-shed cuticles from earlier larval stages at the tail, mid-body and head regions (Figs. 2E, F and G). In nematodes, the new collagen-rich cuticle of each developmental stage is synthesised underneath the existing cuticle, which is subsequently shed during molting. The *pdi-2*-associated molt defects manifest themselves in various forms, ranging from a constriction in the mid-body region (Fig. 2E and F) to a retained sheath of cuticle attached to the nematode tail (Figs. 2E and G). As a direct consequence of the extreme fragility associated with the mutant cuticle many of the

13

pdi-2 homozygotes ruptured during preparation for light microscopy, a feature not observed in any of the other strains examined. Scanning electron microscopy (SEM) and transmission EM (TEM) were applied to examine the cuticle surface and structure in more detail. The outermost layer of the wild type adult cuticle is patterned with evenly spaced (1µm apart) circumferential rings, or annular furrows, and three longitudinal ridges termed alae (Figs. 2I). SEM revealed that the cuticles of the *pdi-2* homozygotes were severely disrupted, displayed irregular folds, smooth patches and were completely devoid of alae (Fig. 2J). The two mutant alleles of *pdi-2* were virtually identical, whereas the cuticles of the *pdi-1* and *pdi-3* homozygotes resembled the wild type cuticle at the SEM level (data not shown). Longitudinal TEM sections of the wild type adult cuticle revealed the electron-dense, highly ordered cuticle with regular surface indentations that corresponded to the annular furrows (Cox et al., 1981) (Fig. 2K). The cuticles of the adult stage *pdi-2* homozygotes were severely disrupted; highly folded and lacked the electron dense matrix material found in the wild type cuticle (Fig. 2L).

The cuticle collagens are disrupted in *pdi-2* mutants. The mutant phenotypes described were consistent with a function for PDI-2 in ECM formation. The role that the PDIs play in the biogenesis of the cuticular ECM was therefore examined by immunocytochemistry with a monoclonal antibody reactive against the cuticle collagen DPY-7 (McMahon et al., 2003). Throughout development DPY-7 localises to the furrows that define the annuli in the wild type cuticle (Fig. 3A). In agreement with gross morphology, staining of *pdi-1* and *pdi-3* mutants with DPY-7 antibody (Figs. 3C and G, respectively) was comparable to wild type (Fig. 3A), having evenly spaced narrow bands. In contrast, DPY-7 localisation in the *pdi-2* strains is severely disrupted indicating that collagen deposition is decreased, with

14

small regions of staining occurring, if at all, in a fraction of the furrows (Fig. 3E).

This result is consistent with the features observed on the adult cuticle of the mutants

at the SEM and TEM levels (Figs. 2J and L).

The complete removal of collagen P4H activity results in embryonic

lethality. Previous reports concluded that the complete removal of collagen P4H

function in *C. elegans* caused lethality during late embryonic development (Winter

and Page, 2000), and biochemical analysis demonstrated that PDI-2 was the sole β

subunit for all P4H complexes in this species (Myllyharju et al., 2002). As would be

predicted from these findings, *pdi-2* RNAi also resulted in embryonic lethality, the

timing and appearance of which was strikingly similar to the combined removal of

active α subunit function (Friedman et al., 2000; Winter and Page, 2000). Due to the

central importance of the P4H null phenotype to the interpretation of *pdi* function, and

to examine the apparent discrepancy between the deletion mutant and the more severe

RNAi phenotype of *pdi-2*, the α subunit mutant strains were re-examined in more

detail. A double mutant strain was produced containing null deletion alleles for the

two α subunit encoding genes, *dpy-18* and *phy-2* which would remove all collagen

P4H active complexes (Myllyharju et al., 2002). This strain was maintained with a

genotype of *dpy-18*(*e1096*)*/+*; *phy-2*(*ok177*)*/phy-2*(*ok177*), phenotypically wild type,

and segregated progeny of which 26.6% were dead embryos (n=493). The embryos

developed normally until the elongated L1 body form was attained thereafter they

collapsed, failed to hatch and ultimately died (data not shown), a phenotype

previously obtained following *phy-2* RNAi in a *dpy-18* mutant background or

following *pdi-2* RNAi (Winter and Page, 2000). Genotypes were confirmed following

15

multiplex single worm PCR analysis (not shown). The phenotype from loss of

collagen P4H function was genetically confirmed as embryonic lethal.

The discrepancies between the *pdi-2* RNAi and the *pdi-2* deletion mutant

phenotypes were further assessed following examination of additional RNAi

constructs. The embryonic lethal effect was initially observed following injection of a

full-length *pdi-2* construct (Winter and Page, 2000). However, introduction of this

construct via the bacterial feeding method (Kamath et al., 2003) resulting in a less

severe but morphologically mutant (dumpy) phenotype (data not shown). In addition,

a smaller RNAi construct representing the third exon, when injected, was found to

replicate the larval lethal deletion mutant phenotype (data not shown).

Synthetic lethality of *pdi-3*(*ka1*) with a subset of collagen-associated

mutants. Mutation in the ERp57/60 encoding gene, *pdi-3*, resulted in a very slight

dumpy phenotype. Previous RNAi experiments however, indicated that PDI-3

synthetically played an important role in collagen biogenesis and cuticle integrity

(Eschenlauer and Page, 2003). *pdi-3* RNAi carried out in specific collagen and

collagen modifying enzyme mutant backgrounds resulted in severe dumpy and lethal

phenotypes, specifically with certain alleles of the cuticle collagen *sqt-3* (Eschenlauer

and Page, 2003). Crosses were therefore performed between *pdi-3*(*ka1*) and various

cuticle collagen-related mutants to confirm and extend these findings genetically

(Table 2). A severe phenotype was demonstrated for both *sqt-3*(*e2117*) and *sqt-*

3(*e2924*) alleles in combination with *pdi-3*(*ka1*), but was not for *sqt-3*(*sc63*); *pdi-*

3(*ka1*) (Table 2). The specific nature of this interaction was also confirmed following

the construction of a *pdi-3*(*ka1*); *dpy-7*(*e88*) mutant, which had no additional

phenotype over the collagen mutant alone (Table 2). Further analysis was performed

by generating double genetic mutants of the cuticle collagen *dpy-17*(*e164*) and the

16

collagen processing enzyme *dpy-31*(*e2770*) in combination with *pdi-3*(*ka1*) (Table 2).

Both double mutants were inviable and displayed a dramatic reduction in body length,

being approximately 150µm long (Figs. 4A and B) compared to 1000µm for *pdi-*

3(*ka1*) (Fig. 2D) and approximately 600µm, for *dpy-31*(*e2770*) or *dpy-17*(*e164*) single

mutants (Novelli et al., 2004). The interaction with the P4H collagen enzyme mutant

dpy-18(*e364*), identified in the RNAi analysis (Eschenlauer and Page, 2003), was also

genetically confirmed in this study.

Functional redundancy among members of the *C. elegans* PDI family.

The potential for redundancy in *C. elegans* PDI function was addressed by

constructing double and triple mutants between the *pdi-1, -2* and *-3* deletion strains.

All strains containing *pdi-2*(*tm0689*) were maintained as heterozygotes for this allele

and homozygotes for the additional alleles. The combined strains were genotyped by

PCR (results not shown) and scored as before (Table 3 and Fig. 4). *pdi-1*(*ka3*)*; pdi-*

3(*ka1*) mutants were viable with no increase in severity of the slight dumpy phenotype

associated with the *pdi-3* mutation. At 25°C there was only a slight increase in

severity of body shape defects at low penetrance (not shown). Double mutants of *pdi-*

1 and *-2* were not affected by growth temperature and segregated severe dumpy

progeny that were identical to *pdi-2*(*tm0689*) alone (Table 3 and Fig. 4C). The *pdi-2*

and *-3* double mutants displayed a phenotype that was also indistinguishable from

pdi-2(*tm0689*) at 15 and 20°C (Table 3 and Fig. 4D). However at 25°C, the *pdi-2* and

-3 double mutants segregated as embryonic lethals (Table 3 and Fig. 4E). The triple

mutant produced embryonic lethal progeny at all growth temperatures tested (Table 3

and Fig. 4F). The embryonic lethal phenotypes were virtually indistinguishable from

each other (Fig. 4 E and F) with embryos developing normally through to elongation

then collapsing, losing their vermiform shape and dying, again being reminiscent of

17

the full-length *pdi-2* RNAi injection phenotype (Winter and Page, 2000). These results demonstrate that in combination, the *pdi* gene products are essential for the completion of late embryogenesis.

The analysis of functional redundancy was also extended to include two additional highly homologous *pdi*-like genes from *C. elegans*. C14B9.2 is an ERp72 homologue that was previously reported to produce no phenotype following RNAi (Kamath et al., 2003) or to give a small body size in a RNAi hypersensitive background (Simmer et al., 2003). ERp72 can functionally compensate for ERp57 loss in murine cells (Soldà et al., 2006). B0403.4 is reported to produce larval arrest upon RNAi disruption in an RNAi-hypersensitive strain (Simmer et al., 2003). RNAi of B0403.4 and C14B9.2 was performed at 20 and 25°C in wild type, RNAi-sensitive strains, all single *pdi* mutants and the *pdi-1; pdi-3* double mutant. No additional effects were observed following RNAi treatment with either gene in any of the above strains. B0403.4 RNAi resulted in L1 larval arrest; with the L1s becoming clear, vacuolated but otherwise displaying a wild-type body form, a phenotype however, only noted in the RNAi-sensitive strain (not shown). The reported RNAi phenotype for C14B9.2 (Kamath et al., 2003) was not replicated in this study.

Complementation of the *pdi-2* mutant phenotype requires intact thioredoxin active sites. A transgenic approach whereby a wild type copy of *pdi-2* was reintroduced into the *pdi-2* mutants confirmed that the phenotypes were due soley to the *pdi-2* deletion. This approach also allowed the functional significance of specific regions of *pdi-2* to be addressed following mutation. The wild type expression plasmid contained the *pdi-2* promoter region, the *pdi-2* cDNA with a synthetic intron sequence and the 3'UTR from the *dpy-18* gene (Winter et al., 2003). Site-directed mutagenesis was also applied to create single *a* domain and double *a/a'*

18

domain thioredoxin mutants by replacing the active-site cysteine residues with structurally similar but non-functional serine residues. The expression of the wild type and mutant *pdi* sequences was assessed by transgene specific RT-PCR (see supplementary material) following microinjection of *pdi-2*(*tm0689*)/ *lon-2*(*e678*) animals co-transformed with a GFP marker. Repair of the *pdi-2* mutant phenotype was determined by individually selecting phenotypically wild type GFP positive nematodes which could either be *pdi-2*(*tm0689*)/*lon-2*(*e678*) heterozygotes or rescued *pdi-2*(*tm0689*) homozygotes. For wild type *pdi-2,* this produced lines that appeared to be rescued homozygotes due to the repair of wild type body shape and segregation of progeny. The genotypes of the rescued animals were confirmed as *pdi-2*(*tm0689*) homozygotes by multiplex PCR. This established that re-expression of wild type *pdi-2* was necessary and sufficient for the repair of this mutant phenotype (see supplemental material for details). A proportion (10-15%) of the individuals from the transgenic rescue lines were noted to be sterile. These individuals most probably represent germ-line mosaics, having lost the rescuing array from the germ-line but not the soma, and consequently displayed a wild-type body form but mutant gonad. The distal regions of the gonad arms in these animals were wild type in appearance and contained syncytial nuclei, whereas the following gonad structure was mutant, being highly vacuolated and disorganised (see supplemental material). In addition, protruding vulva and expelled gonad tissues were noted in a proportion of these animals. This implies that the sterility observed in the *pdi-2* mutants may not only be a result of their mutant body shape, thereby suggesting an additional role for PDI-2.

The same transgenic rescue procedure was performed for *pdi-2* single and double thioredoxin site-inactivated constructs, both of which failed to complement the mutant phenotype after multiple attempts. Successful expression of the mutant

transgene was however confirmed for all transgenic lines by RT-PCR (see

supplemental material for details). Western blotting of wild type nematode extracts

with a PDI-2 anti-peptide antibody (Myllyharju et al., 2002) identified a specific band

migrating at 55kDa, corresponding to the predicted molecular weight of PDI-2, in

addition to two lower molecular weight cross-reactive bands (Fig. 5, lane 1). Extracts

from the deletion strain TP69 (Fig. 5, lane 2), and TP91 (data not shown) did not

express the 55kDa PDI-2 specific band but did express the cross-reactive bands.

Transgenic lines carrying PDI-2 active site mutations, which failed to rescue the

mutant body form, did however re-express the PDI-2-specific 55kDa band (Fig. 5,

lanes 3 and 4). As expected, the transgenic lines rescued with wild type *pdi-2* shared

this Western blot profile (Fig. 5, lane 5).

PDI function is conserved between humans and nematodes. Human PDI

and *C. elegans* PDI-2 are predicted to be orthologs, with both being identified as the

collagen P4H complex-forming β subunit in their respective species (Myllyharju and

Kivirikko, 2004). In support of this, *in vitro* studies demonstrated that insect cell co-

expression of the α subunit from one species can assemble with PDI from the other

species to produce active P4H complexes (Myllyharju et al., 2002). The ability of

human PDI to functionally substitute for PDI-2 was assessed by transgenically-

expressing the human gene in the *C. elegans pdi-2* mutant. Mutant homozygotes were

partially rescued by expression of human PDI following standard injection procedures

(result not shown). Rescued homozygotes were however found to be sterile, possibly

due to transgene silencing in the germline, a common feature of *C. elegans*

transgenesis. In order to overcome this, linearized rescue and marker plasmid were re-

injected with random fragments of *C. elegans* genomic DNA, a technique which has

been shown to alleviate transgene silencing in the germline of *C. elegans* (Kelly et al.,

20

1997). Eight transgenic lines were produced following transformation with human

PDI and selected to identify rescued homozygotes as described above. The rescued

animals displayed a relatively wild type body shape (Fig. 6A and B), consistent with a

degree of functional rescue with regards to the molt, severe dumpy and uncoordinated

phenotypes and went on to produce viable progeny. Genotypes of the rescued lines

were confirmed as *tm0689* homozygotes that amplified only the large deletion product

following multiplex PCR (Fig. 6C, lane 1), when compared to the heterozygote and

wild type (N2) controls (Fig. 6C, lanes 2 and 3, respectively). Testing of three

transgenic lines revealed that they all expressed the spliced transgenic product (Fig.

6D, lanes 1-3), compared to the unspliced control or the negative control (Fig. 6D,

lane 4 and lane 5, respectively). In addition, the human *PDI* rescued lines were found

to lose their rescued body form following human *PDI*-specific RNAi thereby

confirming that rescue was being conferred by the human gene (data not shown).

Discussion

      Protein disulfide isomerase is a ubiquitous multifunctional enzyme that plays

essential roles, including the folding and transit of proteins from the ER. The domain

structure has been biochemically characterised and contains disulfide oxidase and

isomerase-specific regions (Kulp et al., 2006). The essential protein folding functions

of thioredoxins and PDIs have been elegantly dissected in *Escherichia coli* and

Saccharomyces cerevisiae (Wilkinson and Gilbert, 2004) and the full protein

structure of yeast Pdi1p has recently been determined (Tian et al., 2006). The full

range of PDI functions in multicellular organisms are however more diverse and

include the role in the P4H collagen modifying complex, an essential enzyme central

to collagen biosynthesis and ECM formation (Myllyharju and Kivirikko, 2004). PDI

21

is also required independently in collagen biogenesis as these molecules in both

vertebrates and nematodes contain disulfide linkages (Bulleid, 1996; Cox et al.,

1981).

In *C. elegans* the wide range of existing mutants alongside the ability to

generate specific gene knockouts and perform RNAi provides the opportunity for

genetic analysis of whole gene families in a single organism. The conserved *pdi*

genes of *C. elegans* were mutated in this study, thereby enabling for the first time an

analysis of the individual and overlapping functions of the conserved PDI family

members in a metazoan. Our results prove that the thioredoxin active sites of PDI-2

are essential for the formation of a normal exoskeleton, affecting body morphology,

movement, larval development and fertility. Together with PDI-1 and PDI-3, this

enzyme is essential for survival beyond late embryogenesis.

PDI-2 is required for normal P4H activity in *C. elegans*. P4H is involved in

an essential early step of collagen biosynthesis where Y position proline residues in

the collagen repeat regions are changed to 4-hydroxyproline, a modification that is

essential for the thermal stability of the mature molecules (Myllyharju and Kivirikko,

2004). All collagen P4H complexes in *C. elegans* are formed from combinations of

the two α subunits, DPY-18 and PHY-2, and PDI-2 (Myllyharju et al., 2002); with

α/PHY subunit solubility and activity being dependant on the presence of PDI

(Myllyharju et al., 2002; Vuori et al., 1992). It would therefore be predicted that loss

of PDI-2 should be identical to loss of P4H activity. This was supported by the

original *pdi-2* RNAi full-length construct that when injected, replicated exactly the

embryonic lethality from combined mutation/RNAi of *dpy-18* and *phy-2* (Winter and

Page, 2000). However as *pdi-2* null mutants were viable beyond embryogenesis, often

developing to adulthood, there was an apparent discrepancy between the severity of

phenotypes arising from the loss of P4H activity and *pdi-2* disruption by RNAi, when compared to the *pdi-2* genetic mutation. The true loss of P4H phenotype was therefore re-examined following the construction of a *dpy-18* and *phy-2* double null mutant, where all collagen P4H complexes would be absent, with the resulting phenotype being embryonic lethality. This result demonstrated that the post-embryonically-viable *pdi-2* mutants must therefore retain some P4H activity. Due to the limitations imposed by the nature of these strains, insufficient material was available to make a direct biochemical analysis of P4H complexes or activity. These findings can however be interpreted in two ways. Firstly, in the *pdi-2* homozygous mutants, in contrast to the *dpy-18*(*e1096*)*; phy-2*(*ok177*) double mutants, the catalytic α subunits are still present and may be independently partially soluble and active, thereby allowing the *pdi-2* mutants to complete embryogenesis. Alternatively, in the absence of PDI-2, the catalytic α subunits may require PDI-1 and PDI-3 for partial activity. However, *in vitro* studies suggest that PDI-1 and -3 cannot act as true P4H complex subunits (Myllyharju et al., 2002) (A. Page, unpublished observations) and may therefore provide a chaperone-like function in this situation. In the first scenario the lethal effects of the combined *pdi* mutation described herein would be independent of P4H function, whereas the second model would involve a P4H-dependant role. It is interesting to note that full-length *pdi-2* double stranded RNA, when microinjected, resulted in embryonic lethality but phenocopied the deletion mutant when introduced via bacterial feeding. In addition, injection of a shorter, exon three specific, *pdi-2* construct was also found to mimic the deletion mutant. These observations may either be the result of a weaker RNAi effect or support the hypothesis that cross-interference is occurring with the injected full-length construct. An alternative explanation is that a significant maternal contribution of functional PDI-2, to the *pdi-2*(null) homozygous

23

embryos, from their *pdi-2/+* heterozygous mothers allows them to undergo embryogenesis. Such a maternal contribution would be eliminated from the embryonically lethal *pdi-2* RNAi worms.

The disulfide isomerase activity of PDI-2 is essential for nematode development. PDI is required within the P4H complex to maintain the α subunits in a catalytically active soluble conformation and enzymatic inactivation of human PDI, via mutation of a single cysteine in one or both of the *a/a'* active sites, does not affect its ability to form fully active P4H complexes (Vuori et al., 1992). Using a similar approach, whereby both active site cysteines of the *a* domain or all four cysteines in the *a/a'* domains were mutated to serine, the nematode PDI-2 was investigated to establish the relative importance of disulfide isomerase and P4H-dependant roles of PDI. Analysis of the mutants in this study together with previous *in vitro* studies (Myllyharju et al., 2002) indicated that PDI-2 is the single primary β subunit for P4H, with deletion of this gene producing severe developmental abnormalities. Re-expression of wild type *C. elegans* PDI-2 from a transgenic array rescued this mutant phenotype, however neither single N-terminal *a* domain or double *a* and *a'* active site PDI mutants provided any degree of phenotypic rescue but they did express correctly folded PDI-2. It was recently hypothesized that the C terminal *a'* domain is involved in disulfide oxidation while the N-terminal domain is involved in disulfide isomerisation (Kulp et al., 2006). From the mutation studies in human PDI (Vuori et al., 1992), transformation of the *pdi-2* mutant strain with enzymatically inactive PDI was expected to return full P4H activity to the mutant. However due to scarcity of material from these mutants this assumption was not confirmed *in vivo*. PDI-2 therefore represents an essential enzyme that may be required for both P4H-dependant function and disulfide isomerase activity.

The *pdi-2* mutant phenotype confirms a role in the biogenesis of the collagenous cuticle. Analysis of the *pdi-2* mutant phenotype both in terms of body morphology and at the level of individual collagens is consistent with PDI-2 playing a key role in the biogenesis of the nematode cuticle collagens. The mutants were severely dumpy, exhibited poor motility, had weakened cuticles, irregular cuticle surface and structural morphology, molt defects and displayed severely disrupted DPY-7 collagen expression in their cuticles. A similar range of defects are typically associated with mutations in critical enzymes that modify, fold and process the collagens required for proper formation of the nematode cuticle (Page and Winter, 2003). This structure is predominantly composed of extensively disulfide linked collagens (Cox et al., 1981), of which the genome encodes over 170 members, each containing three clusters of conserved cysteine residues (Page and Winter, 2003). The C-terminal cysteines may form disulfide bonds between monomeric collagen chains and thereby nucleate the zipper-like triple helix formation. Alternatively, disulfide interactions may occur between collagen trimers, or indeed at the level of the higher order structure formation. Mutations in conserved C-terminal cysteine residues in the SQT-1 cuticle collagen result in abnormal nematode body morphologies (Kramer and Johnson, 1993). In addition, the transgenic expression of SQT-1 and the related collagen ROL-6 cysteine substitution mutant, generated similar morphologically mutant phenotypes (Yang and Kramer, 1994). The phenotypes observed were however distinct from the essentially wild type loss-of-function phenotypes, suggesting that the mutant proteins did in fact trimerize and become incorporated into the cuticle. Thus the conserved C-terminal cysteine residues are required for normal function but not for trimer assembly, perhaps indicating that the disulfide links are required for inter-trimer interactions and it is this function that may be provided by

25

the disulfide oxidase and isomerase activity of PDI-2. A similar model for vertebrate

collagen assembly has been proposed, where intermolecular disulfide bonding is

thought to stabilize the assembled collagen but is not required for either monomer

association or trimerization (Bulleid et al., 1996). The role that PDI-2 plays in cuticle

collagen assembly is also highlighted by the transmission electron micrographs of the

pdi-2 homozygous mutant cuticle, a structure that was devoid of electron-dense

material (Fig. 2I) and was remarkably similar in appearance to the wild type cuticle

following extraction with a sulfydryl reducing agent (Cox et al., 1981).

An ECM-related function is further supported through the synthetic

lethal phenotype of the conserved PDIs. All three PDIs share a similar cyclical

temporal profile and are localised to the collagen-synthesising hypodermis

(Eschenlauer and Page, 2003; Page, 1997; Winter and Page, 2000). The synergistic

phenotype associated with the *pdi* mutants is consistent with an overlap of functions

in vivo and is compatible with a shared role in collagen biogenesis. The *pdi* triple

homozygote and the temperature sensitive *pdi-3*(*ka1*); *pdi-2*(*tm0689*) double mutants

were embryonic lethal. This result also supports the hypothesis that the *pdi-2* RNAi

embryonic lethality (Winter and Page, 2000) was a consequence of cross-interference

of *pdi-1* and *-3* in addition to the primary target.

The synthetic lethality following RNAi of *pdi-3* described previously

(Eschenlauer and Page, 2003) was confirmed genetically in this study. The synthetic

larval death and severe body morphology defects found for the *pdi-3*(*ka1*) deletion

mutant was highly specific to two key cuticle collagen genes, SQT-3 and DPY-17, the

P4H α subunit encoding gene DPY-18 and the pro-collagen C-peptidase DPY-31. The

in vivo assembly of the SQT-3 protein is dependent on DPY-17, and *vice versa*, with a

model suggesting an intracellular association between DPY-17 and SQT-3 collagen

26

homotrimers (Novelli et al., 2006). SQT-3 has been identified as the major substrate of the proteinase DPY-31 that is required to process pro-collagen into its mature form (Novelli et al., 2004). In support of this interaction, mutants of either *dpy-17* or *dpy-31* in combination with *pdi-3(ka1)* resulted in specific synthetic lethality with associated extreme body morphology defects. It is also significant to note that both *sqt-3(e2117)* and *dpy-31(e2770)* are temperature sensitive lethal alleles, with lethality occurring at a lower temperature in combination with *pdi-3(ka1)*. Furthermore, both SQT-3 and DPY-17 represent excellent substrates for the P4H enzyme encoded by *dpy-18*. The specific function of PDI-3 remains to be elucidated, however in addition to disulfide isomerase activity, PDI-3 has been shown to possess transglutaminase-like activity that may be involved in the cross-linking of the cuticle components and the formation of higher order structures (Eschenlauer and Page, 2003). Vertebrate ERp57, the homologue of PDI-3, in association with calnexin and calreticulin is involved in glycoprotein-specific quality control in the ER (Oliver et al., 1997) and a similar chaperone-type role may additionally be envisaged for PDI-3.

Evolutionary conservation of PDI function. It is interesting to note, that in spite of the fact that PDI-2 plays many nematode- and indeed cuticle-specific functions in *C. elegans,* there is a high degree of conservation of function to man. The human *PDI* gene was able to rescue the *C. elegans pdi-2* mutant phenotype, a function not conferred by the paralogous genes *pdi-1* and *-3*. This confirms that some of the major functions performed by PDI in man include its role in the P4H complex, its disulfide isomerase activity and its ability to modify and assemble critical ECM components such as the ubiquitous collagens.

27

References

Barstead, R.J., 1999. Reverse genetics. In: Hope, I. A. (Ed), *C. elegans*: a practical approach. Oxford University Press, Oxford, UK, pp. 97-118.

Bulleid, N.J., 1996. Novel approach to study the initial events in the folding and assembly of procollagen. Semin. Cell Dev. Biol. 7**,** 667-672.

Bulleid, N.J., Wilson, R., Lees, J.F., 1996. Type-III procollagen assembly in semi-intact cells: chain association, nucleation and triple-helix folding do not require formation of inter-chain disulphide bonds but triple-helix nucleation does require hydroxylation. Biochem. J. 317**,** 195-202.

Cox, G.N., Kusch, M., Edgar, R.S., 1981. Cuticle of *Caenorhabditis elegans*: its isolation and partial characterisation. J. Cell Biol. 90**,** 7-17.

Cox, G.N., Staprans, S., Edgar, R.S., 1981. The cuticle of *Caenorhabditis elegans* II. Stage-specific changes in ultrastructure and protein composition during postembryonic development. Dev. Biol. 86**,** 456-470.

Darby, N.J., Penka, E., Vincentelli, R., 1998. The multi-domain structure of protein disulfide isomerase is essential for high catalytic efficiency. J. Mol. Biol. 276**,** 239-247.

Ellgaard, L., Ruddock, L.W., 2005. The human protein disulphide isomerase family: substrate interactions and functional properties. EMBO Rep. 6**,** 28-32.

Eschenlauer, S.C.P., Page, A.P., 2003. The *Caenorhabditis elegans* ERp60 homolog PDI-3 has disulphide isomerase and transglutaminase-like cross-linking activity and is involved in the maintainance of body morphology. J. Biol. Chem. 278**,** 4227-4237.

Friedman, L., Higgin, J.J., Moulder, G., Barstead, R., Raines, R.T., Kimble, J., 2000. Prolyl 4-hydroxylase is required for viability and morphogenesis in *Caenorhabditis elegans*. Proc. Natl. Acad. Sci. U. S. A. 97**,** 4736-4741.

Gething, M.J., Sambrook, J., 1992. Protein folding in the cell. Nature 355**,** 33-45.

Goldberger, R.F., Epstein, C.J., Anfinsen, C.B., 1964. Purification and properties of a microsomal enzyme system catalyzing the reactivation of reduced ribonuclease and lysozyme. J. Biol. Chem. 239**,** 1406-1410.

Johnstone, I.L., Barry, J.D., 1996. Temporal reiteration of a precise gene expression pattern during nematode development. EMBO J. 15**,** 3633-3639.

Kamath, R.S., Fraser, A.G., Dong, Y., Poulin, G., Durbin, R., Gotta, M., Kanapin, A., Le Bot, N., Moreno, S., Sohrmann, M., Welchman, D.P., Zipperlen, P., Ahringer, J., 2003. Systematic functional analysis of the *Caenorhabditis elegans* genome using RNAi. Nature 421**,** 231-237.

Kelly, W.G., Xu, S.Q., Montgomery, M.K., Fire, A., 1997. Distinct requirements for somatic and germline expression of a generally expressed *Caernorhabditis elegans* gene. Genetics 146**,** 227-238.

Kemmink, J., Darby, N.J., Dijkstra, K., Nilges, M., Creighton, T.E., 1997. The folding catalyst protein disulfide isomerase is constructed of active and inactive thioredoxin modules. Curr. Biol. 7**,** 239-245.

Kimble, J., Ward, S., 1988. In: Wood, W.B. (Ed), The nematode *Caenorhabditis elegans* germ-line development and fertilization. Cold Spring Harbor Laboratory, New York, NY, 191-213.

Koivunen, P., Helaakoski, T., Annunen, P., Veijola, P., Veijola, J., Raisanen, S., Pihlajaniemi, T., Kivirikko, K.I., 1996. ERp60 does not substitute for protein disulphide isomerase as the β-subunit of prolyl 4-hydroxylase. Biochem. J. 316**,** 599-605.

Koivunen, P., Salo, K.E.H., Myllyharju, J., Ruddock, L.W., 2005. Three binding sites in protein-disulfide isomerase cooperate in collagen prolyl 4-hydroxylase tetramer assembly. J. Biol. Chem. 280**,** 5227-5235.

Kramer, J.M., 1997. Extracellular matrix. In: Riddle, D. L., Blumenthal, T., Meyer, B. J., Priess, J. R. (Eds), *C. elegans* II, Cold Spring Harbour Laboratory Press, Cold Spring Harbour, NY, pp. 471-500.

Kramer, J.M., Johnson, J.J., 1993. Analysis of mutations in the *sqt-1* and *rol-6* collagen genes of *Caenorhabditis elegans*. Genetics 135, 1035-1045.

Kulp, M.S., Frickel, E.M., Ellgaard, L., Weissman, J.S., 2006. Domain architecture of protein-disulfide isomerase facilitates its dual role as an oxidase and an isomerase in Ero1p-mediated disulfide formation. J. Biol. Chem. 281, 876-884.

McMahon, L., Muriel, J.M., Roberts, B., Quinn, M., Johnstone, I.L., 2003. Two sets of interacting collagens form functionally distinct sub-structures within the *C. elegans* extracellular matrix. Mol. Biol. Cell 14, 1366-1378.

Myllyharju, J., Kivirikko, K.I., 2004. Collagens, modifying enzymes and their mutations in humans, flies and worms. Trends Genet. 20, 33-43.

Myllyharju, J., Kukkola, L., Winter, A.D., Page, A.P., 2002. The exoskeleton collagens in *Caenorhabditis elegans* are modified by prolyl 4-hydroxylase with unique combinations of subunits. J. Biol. Chem. 277, 29187-29196.

Novelli, J., Ahmed, S., Hodgkin, J., 2004. Gene interactions in *Caenorhabditis elegans* define DPY-31 as a candidate procollagen C-proteinase and SQT-3/ROL-4 as its predicted major target. Genetics 168, 1259-1273.

Novelli, J., Page, A.P., Hodgkin, J., 2006. The C terminus of collagen SQT-3 has complex and essential functions in nematode collagen assembly. Genetics 172, 2253-2267.

Oliver, J.D., van der Wal, F.J., Bulleid, N.J., High, S., 1997. Interaction of the thiol-dependent reductase ERp57 with nascent glycoproteins. Science 275, 86-88.

Page, A.P., 1997. Cyclophilin and protein disulphide isomerase genes are co-transcribed in a functionally related manner in *Caenorhabditis elegans*. DNA Cell Biol. 16, 1335-1343.

Page, A.P., Hamilton, A.J., Maizels, R.M., 1992. *Toxocara canis*: monoclonal antibodies to carbohydrate epitopes of secreted (TES) antigens localize to different secretion-related structures in infective larvae. Exp. Parasitol. 75, 56-71.

Page, A.P., Winter, A.D., 2003. Enzymes involved in the biogenesis of the nematode cuticle. Advances in Parasitology 53**,** 85-148.

Pirneskoski, A., Klappa, P., Lobell, M., Williamson, R.A., Byrne, L., Alanen, H.I., Salo, K.E.H., Kivirikko, K.I., Freedman, R.B., Ruddock, L.W., 2004. Molecular characterization of the principal substrate binding site of the ubiquitous folding catalyst protein disulfide isomerase. J. Biol. Chem. 279**,** 10374-10381.

Pirneskoski, A., Ruddock, L.W., Klappa, P., Freedman, R.B., Kivirikko, K.I., Koivunen, P., 2001. Domains *b'* and *a'* of protein disulfide isomerase fulfill the minimum requirement for function as a subunit of prolyl 4- hydroxylase. The N-terminal domains *a* and *b* enhance this function and can be substituted in part by those of ERp57. J. Biol. Chem. 276**,** 11287-11293.

Simmer, F., Moorman, C., van der Linden, A.M., Kuijk, E., van den Berghe, P.V.E., Kamath, R.S., Fraser, A.G., Ahringer, J., Plasterk, R.H.A., 2003. Genome-wide RNAi of *C. elegans* using the hypersensitive *rrf-3* strain reveals novel gene functions. Plos Biology 1**,** 77-84.

Soldà, T., Garbi, N., Hämmerling, G.J., Molinari, M., 2006. Consequences of ERp57 deletion on oxidative folding of obligate and facultative clients of the calnexin cycle. J. Biol. Chem. 281**,** 6219-6226.

Tian, G., Xiang, S., Noiva, R., Lennarz, W.J., Schindelin, H., 2006. The crystal structure of yeast protein disulfide isomerase suggests cooperativity between its active sites. Cell 124**,** 61-73.

Veijola, J., Annunen, P., Koivunen, P., Page, A.P., Philajaniemi, T., Kivirikko, K.I., 1996. Baculovirus expression of two protein disulphide isomerase isoforms from *Caenorhabditis elegans* and characterisation of prolyl 4-hydroxylases containing one of these polypeptides as their β subunit. Biochem. J. 317**,** 721-729.

Vuori, K., Pihlajaniemi, T., Marttila, M., Kivirikko, K.I., 1992. Characterization of the human prolyl 4-hydroxylase tetramer and its multifunctional protein disulfide isomerase subunit synthesized in a baculovirus expression system. Proc. Natl. Acad. Sci. U. S. A. 89**,** 7467-7470.

Vuori, K., Pihlajaniemi, T., Myllylä, R., Kivirikko, K.I., 1992. Site-directed mutagenesis of human protein disulfide isomerase: effect on the assembly,

activity and endoplasmic reticulum retention of human prolyl 4-hydroxylase in *Spodoptera frugiperda* insect cells. EMBO J. 11**,** 4213-4217.

Wilkinson, B., Gilbert, H.F., 2004. Protein disulfide isomerase. Biochimica Et Biophysica Acta-Proteins And Proteomics 1699**,** 35-44.

Winter, A.D., Myllyharju, J., Page, A.P., 2003. A hypodermally expressed prolyl 4-hydroxylase from the filarial nematode *Brugia malayi* is soluble and active in the absence of protein disulphide isomerase. J. Biol. Chem. 278**,** 2554-2562.

Winter, A.D., Page, A.P., 2000. Prolyl 4-hydroxylase is an essential procollagen-modifying enzyme required for exoskeleton formation and the maintenance of body shape in the nematode *Caenorhabditis elegans*. Mol. Cell. Biol. 20**,** 4084-4093.

Yang, J., Kramer, J.M., 1994. *In vitro* mutagenesis of *Caenorhabditis elegans* cuticle collagens identifies a potential subtilisin-like protease cleavage site and demonstrates that carboxyl domain disulfide bonding is required for normal function but not assembly. Mol. Cell. Biol. 14**,** 2722-2730.

Figure Legends

Figure 1. Domain structure of conserved PDIs from *Caenorhabiitis elegans.* Thioredoxin (*a* and *a'*) active sites (CxxC), N-terminal signal peptides (arrowed) and C-terminal ER retention sequences (H/K T/E EL) are depicted. Relative positions of deletion mutations *ka3*, *gk375, tm0689* and *ka1* are shown.

Figure 2. Body morphology phenotypes of *pdi* mutant nematodes. (A) Wild type *C. elegans* strain N2 (1125µm long). (B) *pdi-1*(*ka3*) viable homozygote adult showing essentially wild type body shape (1041µm long). (C) *pdi-2*(*tm0689*) adult stage. These nematodes were inviable, extremely dumpy and sterile (390µm long). (D) *pdi-3*(*ka1*) viable homozygote adult displaying slight dumpy phenotype (1000µm long). For Nomarski images A-D the scale bar represents 100µm. (E to H) Nomarski images of *pdi-2*(*tm0689*) homozygotes (scale bars represent 25µm), with the black arrows indicating unshed cuticle and a body constriction due to defects in molting, hatched lines the position of the displaced gonad, while an asterisk denotes the vulva. In panel G a comparison of the severely mutant adult stage (upper animal) to the L4 larval stage (lower animal) *pdi-2*(*tm0689*) is depicted. Scanning electron micrographs of the cuticle of wild type N2 and *pdi-2*(*tm0689*) severe dumpy adults, (I and J) respectively. Black arrows depict circumferential annular furrows that separate a single annulus, and white arrow one of the three lateral alae. Scale bars represent 10µm. TEM of a longitudinal section the wild type N2 cuticle (K) compared to a *pdi-2*(*tm0689*) severe dumpy adult cuticle (L). Black arrows depict the annular furrows of a single annulus and the asterisk denotes the cuticle synthesising hypodermis. Scale bars represent 1µm.

33

Figure 3. DPY-7 collagen immunolocalization in wild type and mutant nematode strains. (A and B) The regular annular furrow staining pattern in wild type N2 strain. (C and D) Regular annular furrow staining in *pdi-1*(*ka3*). (E and F) Fragmented severely disrupted annular furrow staining in *pdi-2*(*tm0689*). (G and H) Regular annular furrow staining in *pdi-3*(*ka1*). (A, C, E and G) viewed by epifluorescence; (B, D, F and H) represent the corresponding Nomarski DIC images. Scale bars represent 10µm.

Figure 4. Synthetic lethal phenotype of *pdi-3(ka1)* in combination with collagen-related mutants, A and B, and phenotypes of combined *pdi* mutants, C-F. (A) *pdi-3*(*ka1*) crossed with cuticle collagen mutant *dpy-17*(*e164*). (B) *pdi-3*(*ka1*) crossed with cuticle collagen modifying enzyme mutant *dpy-31*(*e2770*). Identical larval lethal phenotypes were also found with *pdi-3*(*ka1*) in combination with *sqt-3* cuticle collagen mutant alleles *e2117* and *e2924*. (C) *pdi-1*(*ka3*); *pdi-2*(*tm0689*) homozygotes, phenotype is unchanged from *pdi-2* single mutation and is unaffected by temperature. (D) *pdi-2*(*tm0689*); *pdi-3*(*ka1*) at 20°C is unchanged from *pdi-2* single mutation. (E) Embryonic lethality of *pdi-2*(*tm0689*); *pdi-3*(*ka1*) homozygotes at 25°C. (F) Embryonic lethal *pdi-1*(*ka3*); *pdi-2*(*tm0689*); *pdi-3*(*ka1*) triple mutant homozygotes. Nomarski DIC images, all scale bars represents 25µm.

Figure 5. Analysis of *in vivo* PDI-2 expression from wild type, mutant and transgenic nematodes. Wild type N2 (*lane 1*), *pdi-2*(*tm0689*) (*lane 2*), *pdi-2*(*tm0689*) transformed with PDI-2 single active site mutant (*lane 3*), with double active site mutant (*lane 4*) and *pdi-2*(*tm0689*) rescued with wild type PDI-2. Nematodes were homogenized in buffer containing 1% SDS, 0.125M tris PH 6.8, 5% β-mercaptoethanol and were

analyzed by SDS PAGE followed by Western blotting using antibodies against PDI-2. The position of the specific PDI-2 reactive band is arrowed.

Figure 6. Complementation of *C. elegans pdi* mutant with human *PDI*. Repair of *tm0689* body morphology defects following transgenic expression of human *PDI*. (A) Representative Nomarski image and (B) corresponding epifluorescent image of the marker transgene in the rescued animal. Scale bars represent 60µm (C) Representative genotyping PCR from one rescued line (*lane 1*) displaying homozygosity for *tm0689* deletion compared to TP69 heterozygote (*lane 2*), wild type N2 (*lane 3*) and negative control lacking template (*lane 4*). An identical profile was shared for all eight transgenic lines. (D) Analysis of transgenic human *PDI* expression by RT-PCR using primers that span the 50 bp synthetic intron sequence. Lanes 1-3 show expression of smaller spliced product in three transgenic lines compared to unspliced product from the rescue plasmid (*lane 4*), neither product was expressed in the genetic background strain TP69 (*lane 5*).

Table 1
Single *pdi* mutant strains.

Growth temperature	Percentage unhatched embryos			
	Percentage mutant progeny			
	TP67, *pdi-1*(*ka3*)	TP69, *pdi-2*(*tm0689*)/ *lon-2*(*e678*)	TP91, *pdi-2*(*gk375*)/ *lon-2*(*e678*)	TP66, *pdi-3*(*ka1*)
15°C	0.8	4.3	4.2	0.3
	0	21.6	27.9	0[a]
	n=117	n=139	n=215	n=317
20°C	0	0	0	4.1
	0	24.7	26.0	0[a]
	n=160	n=397	n=365	n=345
25°C	0.7	0.7	1.4	1.2
	0	20.1	21.3	0[a]
	n=133	n=145	n=211	n=329

[a] TP66 nematodes were all slightly dumpy.

Table 2

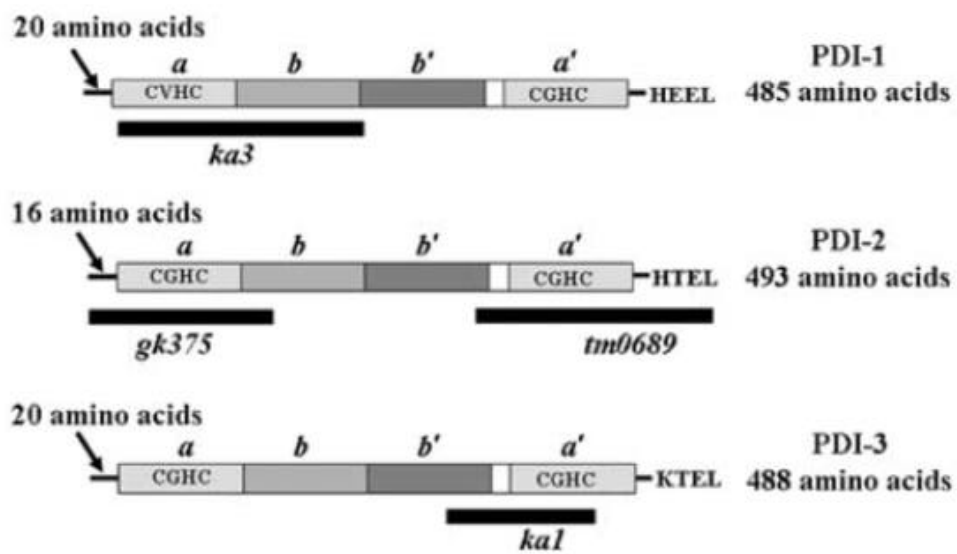*pdi-3*(*ka1*) crosses with specific collagen and collagen enzyme mutants.

Strain	Genotype (gene class)	Phenotype[a]
CB4121	*sqt-3*(*e2117*) V (collagen)	Temperature sensitive lethal, medium dumpy[a] at 15°C
-	*sqt-3*(*e2924*) V (collagen)	Temperature sensitive lethal, medium dumpy at 15°C
CB164	*dpy-17*(*e164*) III (collagen)	Medium dumpy at 15-25°C
CB364	*dpy-18*(*e364*) III (P4H α subunit)	Medium dumpy at 15-25°C
-	*dpy-31*(*e2770*) III (proteinase)	Temperature sensitive lethal, dumpy at 15°C
BE63	*sqt-3*(*sc63*) III (collagen)	Dominant, homozygote weak roller[b] at 15°C
CB88	*dpy-7*(*e88*) X (collagen)	Medium dumpy at 15°C-25°C
TP75	*pdi-3*(*ka1*) I; *sqt-3*(*e2117*) V	Larval lethal at 15°C
TP76	*pdi-3*(*ka1*) I; *sqt-3*(*e2924*) V	Larval lethal at 15°C
TP77	*pdi-3*(*ka1*) I; *dpy-17*(*e164*) III	Larval lethal at 15°C
TP78	*pdi-3*(*ka1*) I; *dpy-18*(*e364*) III	Viable, temperature-dependant severe dumpy
TP79	*pdi-3*(*ka1*) I; *dpy-31*(*e2770*) III	Larval lethal at 15°C
TP94	*pdi-3*(*ka1*) I; *sqt-3*(*sc63*) III	Weak dumpy/roller at 15°C
TP95	*pdi-3*(*ka1*) I; *dpy-7*(*e88*) X	Medium dumpy at 15-25°C

[a]Dumpy, short fat body shape.

[b]Roller, helically twisted body shape.
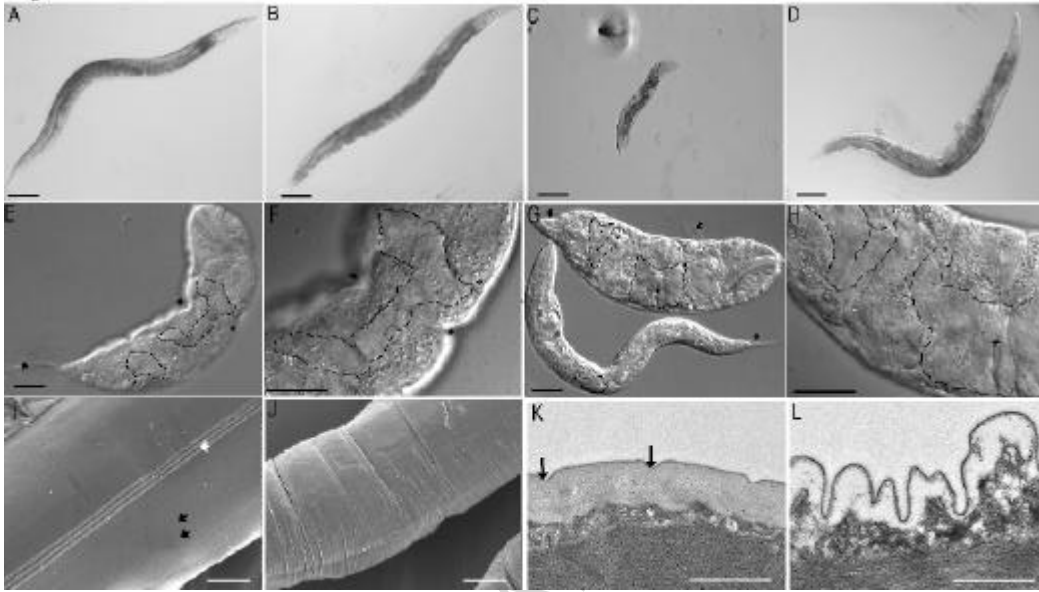
Table 3
Combined *pdi* mutant strains.

Growth temperature	Percentage unhatched embryos			
	Percentage mutant progeny			
	TP72, *pdi-1*(*ka3*); *pdi-3*(*ka1*)	TP84 *pdi-1*(*ka3*); *pdi-2*(*tm0689*)	TP85 *pdi-2*(*tm0689*); *pdi-3*(*ka1*)	TP96 *pdi-1*(*ka3*); *pdi-2*(*tm0689*); *pdi-3*(*ka1*)
15°C	3.0	4.2	3.7	27.7
	0	21.1	22.2	0
	n=33	n=142	n=81	n=372
20°C	0	1.3	4.8	25.0
	0	24.6	18.1	0
	n=71	n=741	n=661	n=192
25°C	2.2	5.5	20.6	25.4
	0	18.3	1.1	0
	n=91	n=327	n=369	n=224

Figure 1

40

Figure 2

41

Figure 3

Figure 4

43

Figure 5